



Article

How Does the Micro-Groove Profile Influence the Mechanics of Taper Junction in Hip Implants? A Finite Element Study

Akash Kalwar, Mohsen Feyzi and Reza Hashemi *

College of Science and Engineering, Flinders University, Tonsley, SA 5042, Australia;
mohsen.feyzi@flinders.edu.au (M.F.)

* Correspondence: reza.hashemi@flinders.edu.au

Abstract: This study aims to investigate the effect of ridged (micro-grooved) surface finish over the trunnion surface on the mechanics (stress, strain, and deformation) of the head–neck taper interface in hip implants. Using finite element modelling, the study focused on the geometric parameters of such micro-grooves to study how they would mechanically affect stress and deformation fields after the assembly procedure. As such, five different 2D models with varying micro-groove height and spacing were produced and assembled under an impaction assembly force of 4 kN in a 32 mm CoCrMo head engaged with a 12/14 Ti-6Al-4V neck. The results showed that lower von Mises stresses could be induced by either an increase or decrease in spacing against the base model (Model 1), which probably signifies that the relationship between the ridge spacing and stress may depend on the level of spacing. It was concluded that the geometrical parameters of the ridges (and their non-linear interactions) impact not only the stress and strain fields but also the assembly loading time at which the maximal stress and plastic deformation occur.

Keywords: micro-grooves; taper junction; hip implants; finite element modelling



Citation: Kalwar, A.; Feyzi, M.; Hashemi, R. How Does the Micro-Groove Profile Influence the Mechanics of Taper Junction in Hip Implants? A Finite Element Study. *Biomechanics* **2023**, *3*, 596–607. <https://doi.org/10.3390/biomechanics3040048>

Academic Editor: Tibor Hortobagyi

Received: 11 September 2023

Revised: 27 November 2023

Accepted: 29 November 2023

Published: 7 December 2023



Copyright: © 2023 by the authors. Licensee MDPI, Basel, Switzerland. This article is an open access article distributed under the terms and conditions of the Creative Commons Attribution (CC BY) license (<https://creativecommons.org/licenses/by/4.0/>).

1. Introduction

Hip replacement surgery is a common treatment for relieving patients of the discomfort induced by damaged hip joint components. This procedure has seen substantial advancement by collecting data and information through analysis of retrieved implants [1,2] and finite element analysis of hip implants [3,4]. Modular metallic and/or ceramic hip implants are used to replace the natural bone structural systems instead of using monoblock implants [5]. The geometry of such implants can be adjusted to the patient's anatomical and physical characteristics, and various components of these implants can be manufactured from various materials, too [1,5]. Even with providing these flexibilities, patients who receive implants may face problematic issues such as implant loosening and premature functional failure due to fretting wear and corrosion at the engaging interfaces of the implants [1,5,6]. Fretting corrosion at the head–neck taper junction causes the release of metallic/ionic debris into the soft tissues in the body, leading to regional tissue reactions, infection, and in some cases, implant failure [6]. Researchers have always been interested in improving the design of such implants and providing recommendations for the assembly procedure, which can, altogether, result in higher interfacial engagement and lower wear, and hence, a better integrity at the head–neck taper junction [7,8].

Finite element analysis (FEA) is one of the commonly used approaches to investigating the strength and integrity of head–neck junctions in hip joint implants. This approach provides an opportunity to play with the design parameters of the implant and shed light on parameters which are difficult to measure in experimental investigations. Although pull-off tests and in vivo analysis are usually conducted, they have multiple limitations in reflecting the complex mechanics of the head–neck interface, and in most cases, they are time-consuming and expensive to conduct. Given these reasons, FEA is preferred by

some researchers for analysing the mechanics of the head–neck junction in a well-replicated virtual environment. The analysis of contact mechanics at the head–neck interface is complex, and the literature confirms that there are many studies to improve the understanding of this interface [7–10]. An FEA study was conducted by Gustafson et al. [10] where a micro-grooved Ti-6Al-4V neck was assembled with a CoCrMo head with various impact forces of 4, 8 and 12 kN. Stress concentration and deformation of the micro-grooves were captured and analysed using FEA.

Previous research has found that various factors such as assembly force, taper angle mismatch, and material combination can significantly affect the strength of the junction [3,4,11,12]. The surface finish of the head and neck components is one of the key parameters affecting the mechanics of the junction. The surface finish parameter has been shown to affect the tribological performance of an interface in simplified pin-on-disk geometries. For instance, Landolt et al. [13] showed that the relative roughness of two contacting bodies can change the mechanical and chemical wear losses from the disk component. Additionally, Kashyap and Ramkumar [14] investigated the influence of micro-groove surface texturing on the tribological performance in a metal-on-polymer pin-on-disk configuration. Several studies, either FEA or retrieval, have been conducted to investigate the mechanics and fretting corrosion in the taper junction of hip implants [7,9,15,16]. In some retrieval studies [16–18], the effect of micro-grooves on the fretting corrosion damage at the junction interface was evaluated. An FEA study conducted by Jauch et al. [19] showed that the stress and strain fields could noticeably be altered with a change in the height of the micro-grooves. It was found that the proportions of the deformed micro-grooves could change from 76% to 100% depending on the height of the micro-grooves. Since the amount of this deformation affects the resulting contact area at the interface, the strength of the interface is expected to change. A retrospective analysis was carried out on 269 head and neck implants obtained from various manufacturers [18]. The study focused on examining fretting corrosion damage in these implants. The results of the analysis indicated that the extent of damage observed in the retrieved implants was correlated with the taper topography [18]. On the other hand, one study conducted by Ashkanfar et al. [7] concluded the negative effect of micro-grooves on the fretting wear of the head–neck junction. They modelled two trunnions: one with a smooth surface and the other as micro-grooved. The two trunnions were then engaged with a 36 mm CoCr head under an assembly force of 4 kN over a period of 0.7 ms. The findings indicated that a smooth taper resulted in a better fixation and lower volumetric wear rate [7]. Based on these studies, there is still inconsistency regarding the role of micro-grooved geometry in the damage of head–neck junctions, as different studies report different results. Taking this into consideration, it is, therefore, still unclear whether or not micro-grooves could improve the mechanical performance of the head–neck junction. Therefore, further investigations are necessary to better understand the mechanics of micro-grooved taper junctions.

Reviewing the literature, several hypotheses have been developed and analysed, including one that an increase in the micro-groove height causes a change in the stress and strain fields at the interface. However, there are still some other important aspects that require further investigations and more understanding. For instance, the change in both the spacing and height of micro-grooves could possibly lead to a non-linear contact behaviour at the interface which can then affect the mechanics of the junction. This necessitates a further analysis of wider variations in the micro-groove profile (depth, height and spacing), as well as the unknown effect of the off-axial assembly procedure together with the material combination on the micro-grooved junctions. In addition, the effect of the micro-groove profile on implant stability is still unknown and requires further research. This paper, therefore, aims to conduct a finite element study on the head–neck junction with varied levels of micro-groove depth and spacing to investigate the influence of micro-groove geometry on the mechanics of the junction. It aims to analyse the role of micro-groove depth and spacing in the stress and strain fields induced at the interface, thereby generating a better picture from the mechanics of micro-grooved junctions.

2. FE Model

A 2D axisymmetric model (Figure 1) was produced for the head–neck junction with the ridged trunnion surface. The analysis aimed to use very small elements at the interface particularly close to the ridges in order to reliably determine the strain of the micro-grooves and the mechanics of the interface.

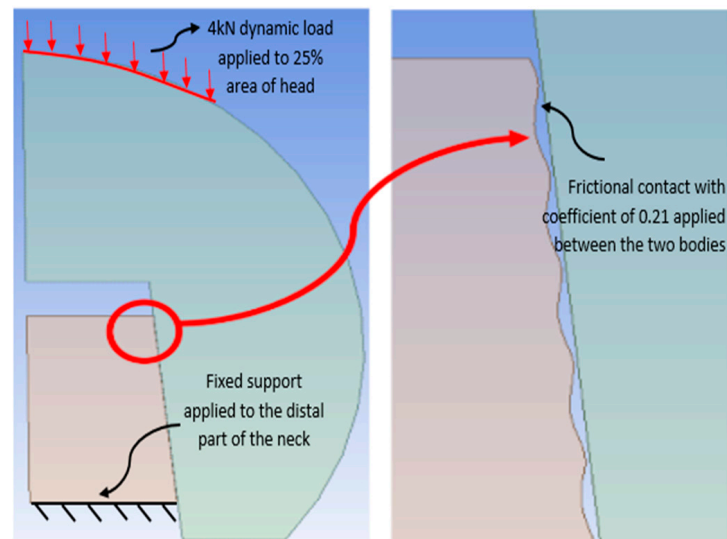


Figure 1. Two dimensional (2D) axisymmetric model with a micro-grooved profile on the neck surface with the boundary conditions and loading applied to the model.

2.1. Model Design

The FEA consisted of two main components, a femoral head, and a neck (trunnion). The design of the head and trunnion was based on dimensions detailed in a previous study [12]. The trunnion was designed with a 12/14 design, a trunnion angle of 5.686 degrees. The 12/14 design refers to a trunnion which has a diameter of 14 mm in its distal end, and 12 mm in the proximal end. A 32 mm head was designed with a taper angle of 5.716 degrees, based on the dimensions available in [12]. The resulted model was of proximal contact with a mismatch angle of 0.015 degrees. There was 1.85 mm between the head's flat roof surface and the trunnion's upper surface [9,12,20].

In total, five different models for the head–neck junction were generated. The head dimensions were the same in all the designs, and the micro-groove height and spacing created on the trunnion's surface were changed among the models. As per the experimental measurements on a micro-grooved neck (CPT, Zimmer, Warsaw, IN, USA), the groove height, depth, and spacing (introduced in Figure 2) were captured as 11 μm , 7 μm , and 200 μm , respectively. These measurements, along with the dimensions of the head and neck components from [12], were employed to create the base model (Model 1). The addition of the micro-grooves was assumed to have no effect on changing the outer diameters of the neck such that a 12/14 neck design was modelled and finalised for the analysis. The three geometrical parameters were then changed in different models, as listed in Table 1. In two models, the height and depth were increased and decreased by 20% while the spacing was kept as constant to the base model. In the other two models, the spacing was changed by 20% while the height and depth were kept the same as the base model. As shown in Figure 2, two different dimensions were considered for height and depth. The profile shape for both the height and depth followed a sinusoidal form.

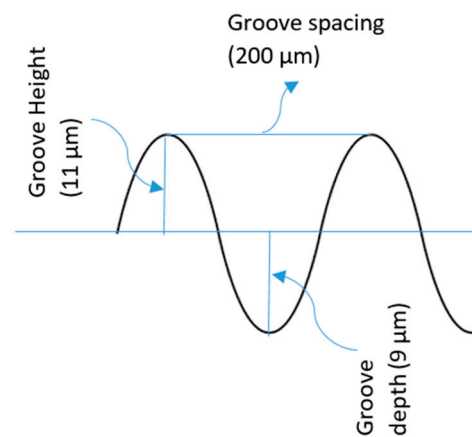


Figure 2. The geometric parameters of the micro-grooved sinusoidal profile on the neck surface.

Table 1. Geometry and dimensions for 5 models with varied micro-groove depth, height, and spacing.

Model Number	Variable(s) for the 2D Models	Micro-Groove Depth (μm)	Micro-Groove Height (μm)	Micro-Groove Spacing (μm)
Model 1	Base model—as per measurements	7	11	200
Model 2	With 20% reduction in depth and height	5.6	8.8	200
Model 3	With 20% increase in depth and height	8.4	13.2	200
Model 4	With 20% reduction in spacing	7	11	160
Model 5	With 20% increase in spacing	7	11	240

2.2. Material Model

A Ti-6Al-4V trunnion was engaged with a Co-28Cr-6Mo femoral head [12]. A multi-linear isotropic hardening plastic model was employed to simulate the material behaviour beyond its elastic limit. Based on these models, the plastic strain was initiated at the yield point, and the material was deemed to have failed at the point where the ultimate tensile strength and percentage of elongation were met. The plastic strain failure was described as the point at which the material's maximum elongation was achieved [12,20]. The models created in SolidWorks were imported into the ANSYS Explicit Dynamics environment and were defined in an axisymmetric configuration. The neck and head components were defined with material properties from Ti and CoCr alloys, respectively (Table 2) [10,20].

Table 2. Material properties used for the two alloys used in the FE modelling.

Material	Young Modulus (GPa)	Poisson's Ratio	Shear Modulus (GPa)	Yield Strength (MPa)	Ultimate Tensile Strength (MPa)	Elongation at Break (%)
Ti-6Al-4V	119	0.29	46.1	840	1020	15
CoCrMo	213	0.30	45.7	930	1310	29

2.3. Meshing and Boundary Conditions

The interaction between the head and neck components was modelled with a friction coefficient of 0.21 [7]. Hex-dominant meshing was used for both the head and neck components [20] and face sizing was applied to their common interface with a refinement factor of 3 for producing reliable results (Figure 3). The process of mesh refinement was

completed a number of times to achieve mesh independent results. The total number of elements for the head and neck components in Model 1 (Table 1) was 117,497 and 111,582, respectively. An explicit dynamics approach was used to replicate the assembly procedure in common surgery.

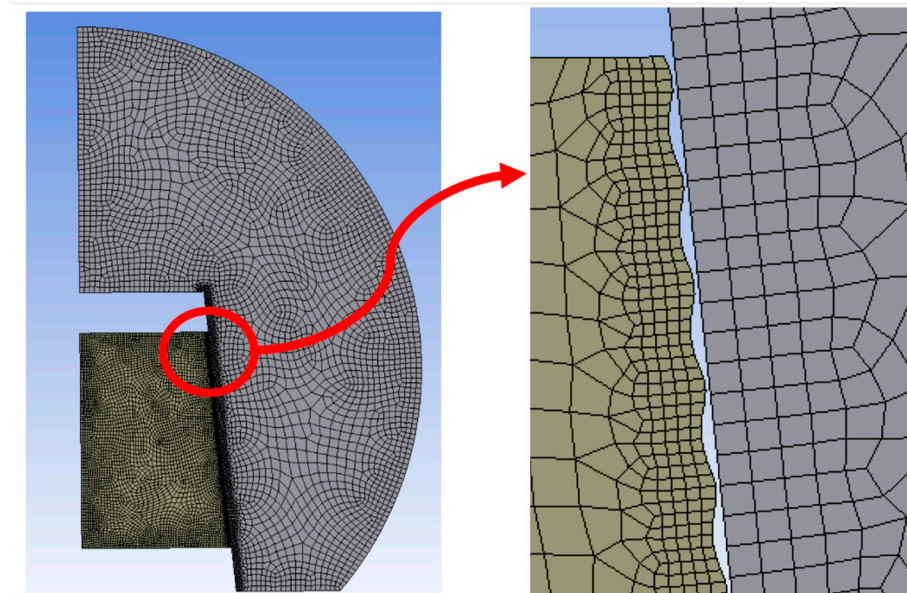


Figure 3. The produced mesh for the head and neck components with detailed meshing close to the ridges.

The total time for the analysis was taken to be 0.001 s. As the time for the load application is around 0.0007 s [3,7], 0.0003 s was applied to provide the settling time. Kinetic energy was monitored during the analysis to ensure that the ratio of kinetic energy to total internal energy would not exceed 10%. The factor that controlled for the quality of solution output was the maximum energy error. This factor stops the solution if the principle of conservation of energy becomes poor.

As for the boundary conditions applied to the model, two boundary conditions were employed to replicate what happens in reality. A force of 4 kN was applied to 25% of the dead diameter [20]. This force was dynamic and varied over a time span of 0.0007 s (as shown in Figure 4) and was followed by a settling time of 0.0003 s.

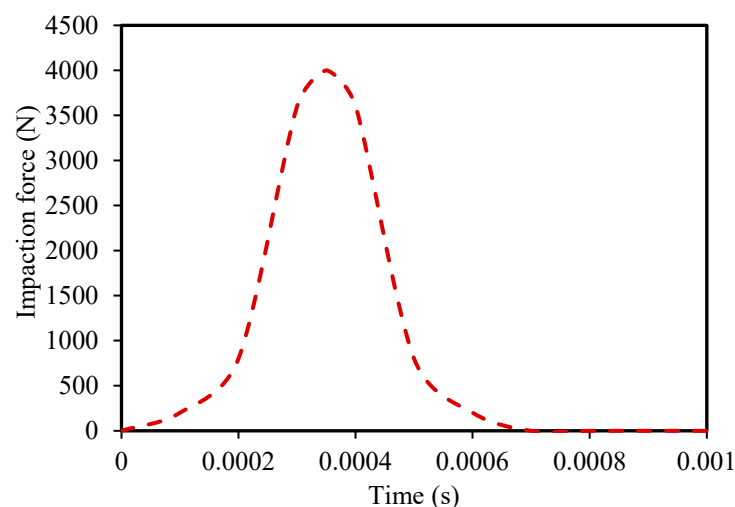


Figure 4. A 4 kN of dynamic assembly force applied to 25% of the head diameter versus the time of application.

3. Results

All the 2D models were simulated with the same methodology so that the effect of ridges could be better understood. The procedure was carried out to analyse and compare the stress, strain, and deformation in different models. The results included the distribution of equivalent stress, shear stress, plastic strain, equivalent elastic strain, shear strain, and directional deformations.

3.1. The Influence of Micro-Groove Height

The results for the stress, strain, and deformations were evaluated for each model. In this study, the results of stress, strain, and deformations of the neck component were included. All the results for the models are graphically illustrated. Figures 5 and 6 illustrate the maximum von Mises stress and maximum plastic strain, respectively for the models with various micro-groove heights.

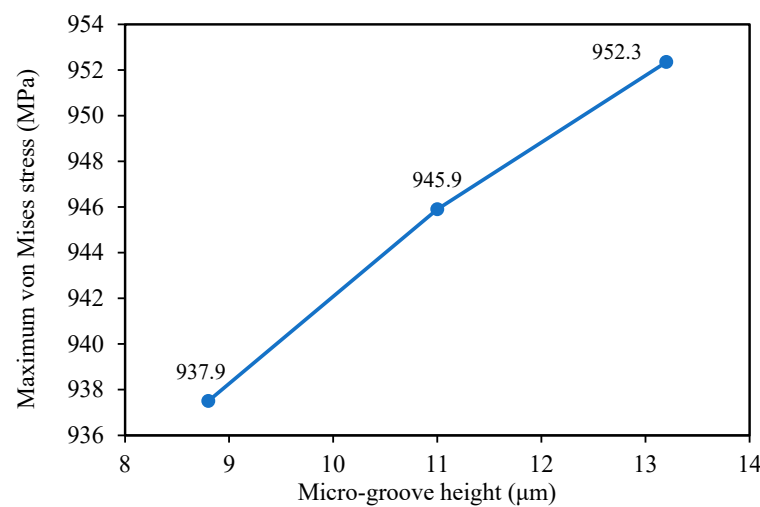


Figure 5. Maximum von Mises stress at the neck surface for various models with change in ridge height.

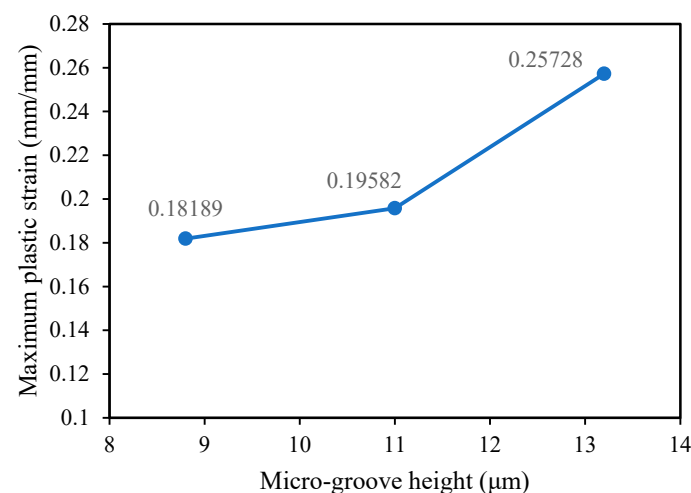


Figure 6. Change in maximum plastic strain with micro-groove height.

An increase in the micro-groove height resulted in an increase in the equivalent von Mises stress increases (Figure 5). For Model 1, the equivalent stress generated at the neck surface was 945.9 MPa. A decrease in the micro-groove height (Model 2) resulted in a decrease in stress to around 937.9 MPa, while an increase in micro-groove height (Model 3) resulted in the stress increasing to 952.4 MPa.

It was observed that with a decrease in the micro-groove height, there was a decrease in maximum plastic strains in Model 2 from 0.19528 to 0.18189 (Figure 6). With an increase in the micro-groove height in Model 3, there was an increase in maximum plastic strain to around 0.25728. The increase in strain in Model 3 was quite sharp when compared with the decrease in maximum strain in Model 2.

3.2. The Influence of Micro-Groove Spacing

A decrease in micro-groove spacing (Model 4) decreased the maximum equivalent stress to 940.3 MPa (Figure 7). However, with an increase in spacing (Model 5), a relatively sharp decrease in stress magnitude was observed (712.5 MPa). This shows the complex effect of the micro-grooved geometry on the mechanics of head-neck junction.

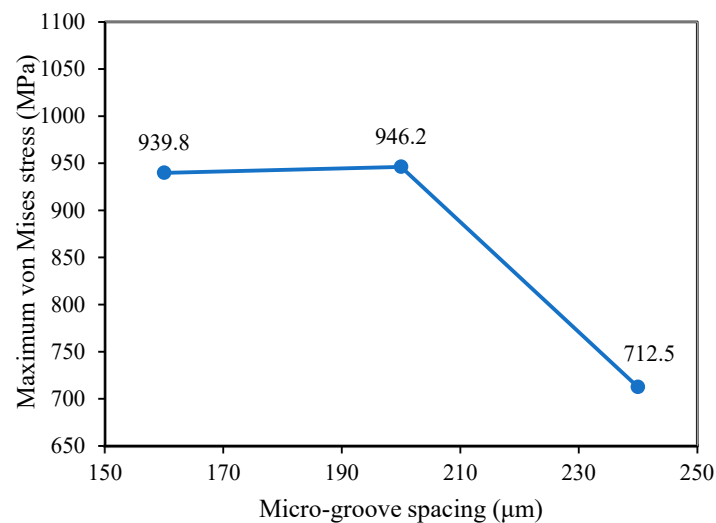


Figure 7. Maximum equivalent von Misses stress over the neck surface with change in the micro-groove spacing.

As shown in Figure 8 for the change in micro-groove spacing, it was observed that a decrease in micro-groove spacing resulted in a sharp increase in plastic strain. Model 5 showed a decrease in plastic strain from 0.1958 to 0.02222, whereas in Model 4 the plastic strain increased from 0.19582 to 0.91182.

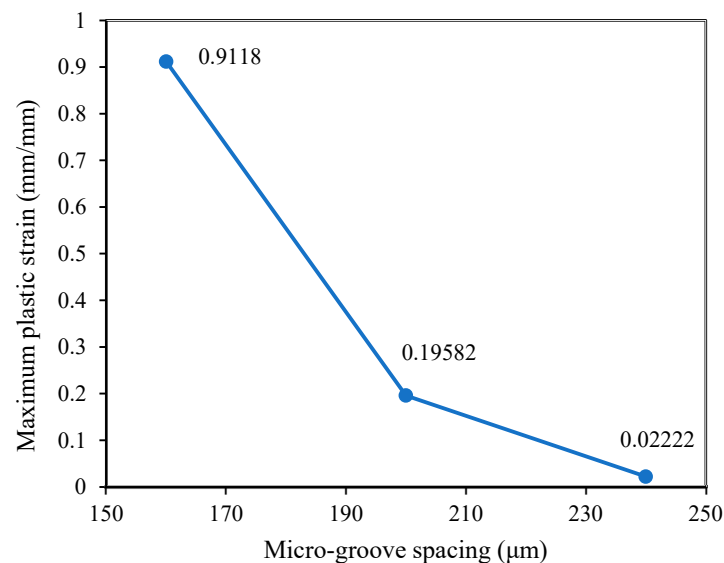


Figure 8. Change in the maximum plastic strain in the neck with change in the micro-groove spacing.

4. Discussion

Modular head–neck junctions provide various advantages such as geometrical adjustments to patients’ specific requirements, and flexibility in material combination and geometrical design parameters. Although being advantageous, this junction has been reported to be associated with fretting corrosion, which ultimately leads to the release of some metallic/ionic particles into the soft tissues around the implant. The stability and strength of such a junction depend on various design parameters such as trunnion geometry, head size, material combination, taper angle mismatch, assembly procedure, and surface finish of the tapered interface. Micro-grooved junctions are traditionally believed to provide a better fixation at the interface by means of plastic deformation at the tip of ridges [3,4,11]. The literature on the micro-grooved junctions is contradictory, such that some studies confirm the traditional view while others question it. This study aimed to analyse the micro-grooved junctions in proximal contact using FEA. A base model was considered for this analysis and the spacing, height, and depth of micro-grooves were changed to evaluate how the micro-groove geometrical parameters may affect the mechanics of the junction. The base model was taken as a reference for comparisons in this study (Model 1). Depending on the design of the base model (Model 1), the effect of the micro-groove depth, height, and spacing on the mechanics of the junction was analysed. As shown in Figure 9, high stresses occurred at the proximal end, which was the result of the initial proximal contact occurring at the taper interface (with a proximal mismatch angle) under the assembly load. Additionally, at the distal end of the trunnion, some high magnitude stresses were observed. This indicated that over the course of assembly loading, the deformation occurring in both of the contacting materials (neck and head) together with the increasing assembly load with time, expanded the contact area towards the distal end. This occurred in the trapezoid-based configuration that existed at the interface of the junction where the applied load was decomposed to normal and tangential load components, resulting in a combined stress state. Under the application of the impaction force of 4 kN, all the micro-grooves on the neck surface were deformed, which was partly consistent with observations by Godoy et al. [15] where 76–100% of the micro-grooves were deformed, depending on the level of assembly force. The difference in the percentages of this study compared with those from Godoy et al. [15] could be attributed to the different micro-groove parameters and materials properties in the two studies.

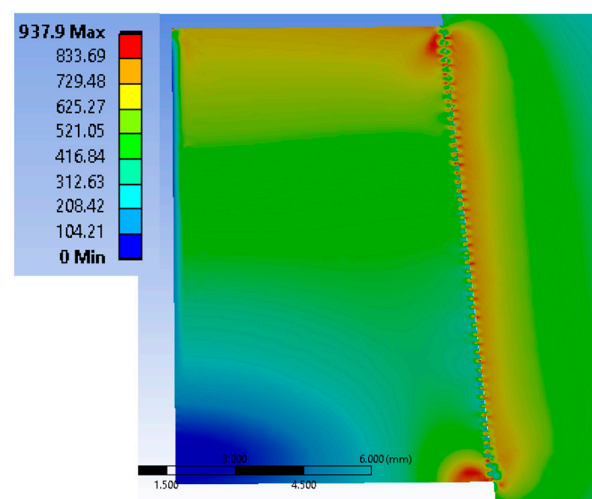


Figure 9. Von Mises stress distribution in both the head and neck contacting region after assembly load (results from Model 2).

As shown in Figure 5, the maximum von Mises stress reduced inconsiderably (by around only 0.8%) between Model 1 and Model 2, from 945.9 to 937.9 MPa. The stresses generated under the impaction force of 4 kN were consistent with those reported in

Gustafson et al. [10]. The percentile increase in maximum von Mises stress from Model 1 to Model 3 was approximately 0.68%. The percentile decrease in the maximum plastic strain from Model 1 to Model 2 was approximately 7%. However, no plastic strain was observed in [9] with even large changes in the geometry of the micro-grooves. An increase in plastic strain between Model 1 and Model 3 was observed, which agreed with the results in Bechstedt et al. [9]. With an increase in the micro-groove height in Model 3, the maximum von Mises stress and maximum plastic strain increased as per Figures 5 and 6, respectively, which showed the proportional influence of the micro-groove height with the von Mises stress and plastic strain. The pattern of the maximum von Mises stress over the length of contact at the interface in all models was similar with different peak values. The results were in agreement with the research conducted by Dransfield et al. [21], Godoy et al. [15] and Bechstedt et al. [9] (each to some degree) and signified the influence of micro-groove geometry in stress and strain generation at the interface. The change in the micro-groove spacing had a different effect than that of the change in height. With a decrease in spacing from Model 1 to Model 4, there was a slight decrease in von Mises stress from 945.9 to 939.8 MP with a percentile decrease of 0.64%. With an increase in spacing from Model 1 to Model 5, the percentile decrease in stress was quite higher at around 24% from 945.9 to 712.5 MPa. These results probably signify that a slight change in the geometry of the micro-grooves could change the mechanics of the junction noticeably. Furthermore, it might be concluded that a decrease in spacing does not always lead to an increase in stress levels, and this influence depends on different parameters such as the value of spacing around which the spacing parameter is changed, the levels of spacing, and complex non-linear contacting interactions occurring at the interface. This can be an interesting subject for future research. As for the plastic strain, the maximum occurred at the tip of the ridges with different magnitudes for various models, however, the pattern of the deformation was similar over the interface between the head and neck components. The plastic strain between Model 1 and Model 4 changed around 365%. There was a significant increase in plastic strain from Model 1 to Model 4. The percentile decrease in plastic strain between Model 1 and Model 5 was approximately around 88%. Hence, there is clear effect of the variation of micro-groove spacing in the stress and strain generation at the neck surface.

Maximum von Mises stress and plastic strain over the time of dynamic load application were monitored and evaluated. With an increase in the impaction force, there was a slight increase in the equivalent stress up to a point where plastic deformation was initiated. The plastic deformation started to increase and became maximum at the time when maximal pressure was applied (0.00035 s). With a decrease in the magnitude of the pressure to zero, it was observed that the equivalent stress did not drop to zero. There was only a slight drop in the stress magnitude and then it became constant (Figure 10). The remaining stress was due to the plastic strains at the tip of the ridges. The somewhat fast change in the maximum von Mises stress occurred for almost all the models, but for each model, it occurred at a different time. A model with higher micro-groove depth was associated with an earlier start of a sharp change in the maximum stress. This is because a model with a smaller micro-groove depth possesses fewer plastic deformations at the tip of its ridges, and this delays the time for the sharp change in the stresses [11]. Similarly, a model with higher spacing causes a delay in the occurrence of a sharp change in the stresses. The von Mises stress generated in the models with different micro-groove depths was consistent with nominal expectations. With an increase in the micro-groove height, there was an increase in the normal stress, and with a decrease in the depth, there was a decrease in the normal stress. With an increase in the spacing, there was a decrease in the von Mises stress as expected; however, with a decrease in the spacing, there was again a decrease in the von Mises stress at the ridges which was inconsistent with the expectations. An increase in spacing, while keeping the height and depth as constant, tends to stretch out the wave-shape profile of the interface. This results in an increase in the contact area; and, therefore, the stress is expected to decrease.

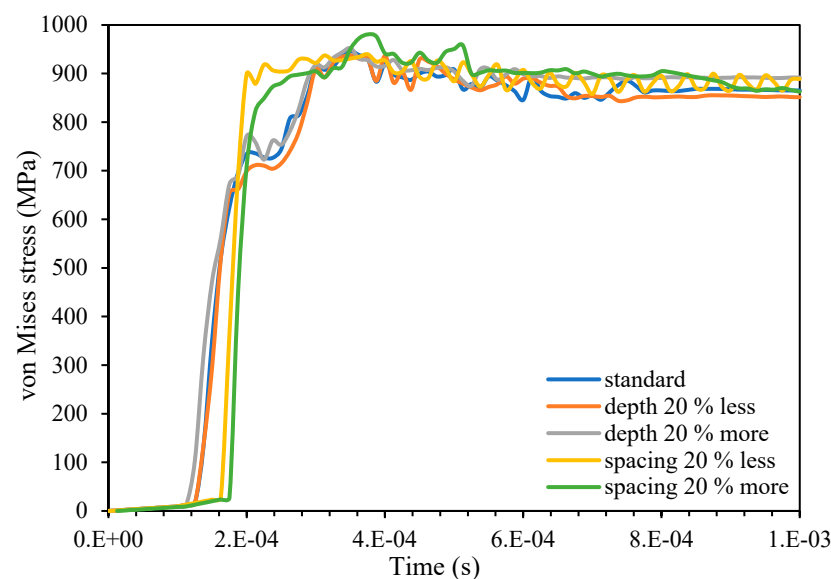


Figure 10. Maximum von Mises stress evolution over the course of force application in different models.

In all the models, close to the distal end, the stress and strain had high magnitudes, which was consistent with the results reported in Bechstedt et al. [9]. With an increase in the micro-groove height, there was an increase in the stress; and a decrease in height resulted in a decrease in equivalent stress, which was consistent with the literature [9]. The difference in the magnitude of stress may be due to the different properties selected for the modelled materials, the approach for the load application and the geometry of the head and neck components. Hence, FEA suggested that micro-grooved geometry affected the stress and strain generation at the interface, as stated by other researchers [15,21].

The scope of this article was limited to studying the mechanics of taper junction in hip implants with a focus on stress, strain, and deformation under dry conditions, in the absence of lubricant (body fluid). This analysis did not include the change in various geometrical parameters such as the taper angle mismatch, assembly force, material combination, different head sizes, and different neck designs. All these parameters affect the mechanics of the junction, especially where these parameters are coupled with the non-linear influence from micro-grooves [3,4]. After the assembly procedure, the taper junction normally undergoes different loading scenarios including walking, stair up and stair down. These loading scenarios can significantly change the stress, strain, and deformation fields at the interface. The inclusion of different geometrical parameters and loading scenarios could be conducted by stochastic FEA to generate a more comprehensive understanding from the effect of micro-grooves on the mechanics of taper junction. This study focused on the stress, strain, and deformation resulting from the assembly load only. These results are not transferrable to the durability of the junction. For instance, higher stresses could reduce micromotions at the interface by increasing the contact area and plastic deformation [22–24]. These can lead to an increase in the stick contacting area which can then reduce the material loss. At the same time, this higher stress can lead to higher material losses in the portion of the contacting area where the slipping occurs [4,25,26]. To explore the clinical relevance of the FEA results, encoded FEA enriched with the progressive damage algorithms are required [27,28]. These algorithms should include complex mechanisms such as fretting corrosion and subsequent material degradation processes at the taper interface. Taking into account the aforementioned limitations, the findings of this study are beneficial in providing a foundation for future analyses of the junction from the mechanical perspective.

5. Conclusions

This study investigated the influence of micro-groove geometry on the mechanics of head–neck junctions in modular hip implants. The height, depth, and spacing of the micro-grooves were selected as variables to explore their influence on the stress, strain, and deformation fields at the head–neck interface. The micro-grooved junctions were associated with higher levels of stress and plastic deformations. The maximum stress occurred at the tip of the ridges and increased with the groove height or spacing. Changes in micro-groove spacing affected plastic deformation, too. There was a clear effect from the ridges in the stress and strain generation at the neck interface during the hip implantation procedure. The behaviour and amount of strain and stress generation clearly depended upon the ridge parameters. The assembly loading time causing maximum stress and plastic deformations depended on the ridge parameters. Further research with the aim of analysing the strength of the joint and pull-off analysis with the inclusion of the spacing influence can be conducted such that an optimal topography for a better strength at the interface could possibly be achieved.

Author Contributions: Conceptualization, R.H. and M.F.; methodology, A.K.; formal analysis, A.K.; investigation, A.K.; resources, R.H.; data curation, A.K.; writing—original draft preparation, A.K.; writing—review and editing, M.F. and R.H.; visualization, A.K.; supervision, R.H. and M.F.; project administration, R.H. All authors have read and agreed to the published version of the manuscript.

Funding: This research received no external funding.

Institutional Review Board Statement: Not applicable.

Informed Consent Statement: Not applicable.

Data Availability Statement: The data for this study are available upon reasonable request.

Conflicts of Interest: The authors declare no conflict of interest.

References

1. Hussenbocus, S.; Kosuge, D.; Solomon, L.; Howie, D.; Oskouei, R.H. Head-neck taper corrosion in hip arthroplasty. *BioMed Res. Int.* **2015**, *2015*, 758123. [[CrossRef](#)] [[PubMed](#)]
2. Oskouei, R.H.; Barati, M.R.; Farhoudi, H.; Taylor, M.; Solomon, L.B. A new finding on the in-vivo crevice corrosion damage in a CoCrMo hip implant. *Mater. Sci. Eng. C* **2017**, *79*, 390–398. [[CrossRef](#)] [[PubMed](#)]
3. Feyzi, M.; Fallahnezhad, K.; Taylor, M.; Hashemi, R. The mechanics of head-neck taper junctions: What do we know from finite element analysis? *J. Mech. Behav. Biomed. Mater.* **2021**, *116*, 104338. [[CrossRef](#)] [[PubMed](#)]
4. Feyzi, M.; Fallahnezhad, K.; Taylor, M.; Hashemi, R. A review on the finite element simulation of fretting wear and corrosion in the taper junction of hip replacement implants. *Comput. Biol. Med.* **2021**, *130*, 104196. [[CrossRef](#)] [[PubMed](#)]
5. Hernigou, P.; Queinnee, S.; Flouzat Lachaniette, C.H. One hundred and fifty years of history of the Morse taper: From Stephen A. Morse in 1864 to complications related to modularity in hip arthroplasty. *Int. Orthop.* **2013**, *37*, 2081–2088. [[CrossRef](#)] [[PubMed](#)]
6. Wight, C.M.; Lanting, B.; Schemitsch, E.H. Evidence based recommendations for reducing head-neck taper connection fretting corrosion in hip replacement prostheses. *Hip Int.* **2017**, *27*, 523–531. [[CrossRef](#)]
7. Ashkanfar, A.; Langton, D.J.; Joyce, T.J. Does a micro-grooved trunnion stem surface finish improve fixation and reduce fretting wear at the taper junction of total hip replacements? A finite element evaluation. *J. Biomech.* **2017**, *63*, 47–54. [[CrossRef](#)]
8. Raji, H.Y.; Shelton, J.C. Prediction of taper performance using quasi static FE models: The influence of loading, taper clearance and trunnion length. *J. Biomed. Mater. Res. Part B Appl. Biomater.* **2019**, *107*, 138–148. [[CrossRef](#)]
9. Bechstedt, M.; Gustafson, J.A.; Mell, S.P.; Gührs, J.; Morlock, M.M.; Levine, B.R.; Lundberg, H.J. Contact conditions for total hip head-neck modular taper junctions with microgrooved stem tapers. *J. Biomech.* **2020**, *103*, 109689. [[CrossRef](#)]
10. Gustafson, J.A.; Pourzal, R.; Levine, B.R.; Jacobs, J.J.; Lundberg, H.J. Modelling changes in modular taper micromechanics due to surgeon assembly technique in total hip arthroplasty. *Bone Jt. J.* **2020**, *102*, 33–40. [[CrossRef](#)]
11. Feyzi, M.; Fallahnezhad, K.; Taylor, M.; Hashemi, R. An Overview of the Stability and Fretting Corrosion of Microgrooved Necks in the Taper Junction of Hip Implants. *Materials* **2022**, *15*, 8396. [[CrossRef](#)] [[PubMed](#)]
12. Fallahnezhad, K.; Farhoudi, H.; Oskouei, R.H.; Taylor, M. Influence of geometry and materials on the axial and torsional strength of the head–neck taper junction in modular hip replacements: A finite element study. *J. Mech. Behav. Biomed. Mater.* **2016**, *60*, 118–126. [[CrossRef](#)] [[PubMed](#)]
13. Landolt, D.; Mischler, S.; Stemp, M. Electrochemical methods in tribocorrosion: A critical appraisal. *Electrochim. Acta* **2001**, *46*, 3913–3929. [[CrossRef](#)]

14. Kashyap, V.; Ramkumar, P. Feasibility study of micro-groove cross hatched surface texturing on Ti6Al4V for improved biotribological performance in metal-on-polymer hip implant. *Tribol.-Mater. Surf. Interfaces* **2019**, *13*, 150–160. [[CrossRef](#)]
15. Godoy, M.; Gustafson, J.A.; Hertzler, J.S.; Bischoff, J.E.; Pourzal, R.; Lundberg, H.J. Model validation for estimating taper microgroove deformation during total hip arthroplasty head-neck assembly. *J. Biomech.* **2022**, *140*, 111172. [[CrossRef](#)]
16. Arnholt, C.M.; Underwood, R.; MacDonald, D.; Higgs, G.; Chen, A.; Klein, G.; Hamlin, B.; Lee, G.; Mont, M.; Cates, H. Micro-Grooved Surface Topography Does Not Influence Fretting Corrosion of Tapers in THA: Classification and Retrieval Analysis. Master's Thesis, Drexel University Philadelphia, Philadelphia, PA, USA, 2015.
17. Arnholt, C.M.; MacDonald, D.W.; Underwood, R.J.; Guyer, E.P.; Rimnac, C.M.; Kurtz, S.M.; Mont, M.A.; Klein, G.R.; Lee, G.-C.; Chen, A.F. Do stem taper microgrooves influence taper corrosion in total hip arthroplasty? A matched cohort retrieval study. *J. Arthroplast.* **2017**, *32*, 1363–1373. [[CrossRef](#)] [[PubMed](#)]
18. Pourzal, R.; Hall, D.J.; Ha, N.Q.; Urban, R.M.; Levine, B.R.; Jacobs, J.J.; Lundberg, H.J. Does surface topography play a role in taper damage in head-neck modular junctions? *Clin. Orthop. Relat. Res.* **2016**, *474*, 2232–2242. [[CrossRef](#)]
19. Jauch-Matt, S.; Miles, A.; Gill, H. Effect of trunnion roughness and length on the modular taper junction strength under typical intraoperative assembly forces. *Med. Eng. Phys.* **2017**, *39*, 94–101. [[CrossRef](#)]
20. Dyrkacz, R.; Brandt, J.; Morrison, J.; O'Brien, S.; Ojo, O.; Turgeon, T.; Wyss, U. Finite element analysis of the head-neck taper interface of modular hip prostheses. *Tribol. Int.* **2015**, *91*, 206–213. [[CrossRef](#)]
21. Dransfield, K.; Racasan, R.; Williamson, J.; Bills, P. Changes in the morphology of microgrooved stem tapers with differing assembly conditions. *Biotribology* **2019**, *18*, 100096. [[CrossRef](#)]
22. Feyzi, M.; Fallahnezhad, K.; Hashemi, R. The effect of key operating parameters on the tribocorrosion of Ti and CoCrMo bio-metals at metal-on-metal contacts. *Tribol. Int.* **2023**, *189*, 108984. [[CrossRef](#)]
23. Feyzi, M.; Fallahnezhad, K.; Taylor, M.; Hashemi, R. The tribocorrosion behaviour of Ti-6Al-4 V alloy: The role of both normal force and electrochemical potential. *Tribol. Lett.* **2022**, *70*, 83. [[CrossRef](#)]
24. Feyzi, M.; Fallahnezhad, K.; Taylor, M.; Hashemi, R. What role do normal force and frequency play in the tribocorrosion behaviour of Ti-6Al-4 V alloy? *Tribol. Int.* **2022**, *172*, 107634. [[CrossRef](#)]
25. Feyzi, M.; Fallahnezhad, K.; Hashemi, R. Tribocorrosion at metal-on-metal contacts: The contributing role of geometry and material combination. *Corros. Sci.* **2023**, *215*, 111047. [[CrossRef](#)]
26. Feyzi, M.; Hashemi, R. Electrochemical current at reciprocating contacts: A new analytical modelling. *Electrochim. Acta* **2023**, *455*, 142460. [[CrossRef](#)]
27. Fallahnezhad, K.; Feyzi, M.; Ghadirinejad, K.; Hashemi, R.; Taylor, M. Finite element based simulation of tribocorrosion at the head-neck junction of hip implants. *Tribol. Int.* **2022**, *165*, 107284. [[CrossRef](#)]
28. Fallahnezhad, K.; Feyzi, M.; Hashemi, R.; Taylor, M. The role of the assembly force in the tribocorrosion behaviour of hip implant head-neck junctions: An adaptive finite element approach. *Bioengineering* **2022**, *9*, 629. [[CrossRef](#)]

Disclaimer/Publisher's Note: The statements, opinions and data contained in all publications are solely those of the individual author(s) and contributor(s) and not of MDPI and/or the editor(s). MDPI and/or the editor(s) disclaim responsibility for any injury to people or property resulting from any ideas, methods, instructions or products referred to in the content.